

# **Mechanical Promotion of Mesenchymal Stem Cell Proliferation and Differentiation Prevents Dietary Induced Obesity While Enhancing Osteogenesis.**

Y. K. Luu<sup>1</sup>, E. Capilla<sup>2</sup>, C. J. Rosen<sup>3</sup>, V. Gilsanz<sup>4</sup>, J. E. Pessin<sup>2</sup>, S. Judex<sup>1</sup> & C. T. Rubin<sup>1†</sup>,

<sup>1</sup> Dept of Biomedical Engineering, Stony Brook University, Stony Brook, NY, USA

<sup>2</sup> Dept of Pharmacological Sciences, Stony Brook University, Stony Brook, NY, USA

<sup>3</sup> The Jackson Laboratory, Bar Harbor, ME, USA

<sup>4</sup> Childrens Hospital of Los Angeles, Los Angeles, CA, USA

**Running Head:** Mechanical Signals Enhance Stem Cell Populations

**Word / Character Count:** 7,677 words / 43,205 characters

**Number of Figures:** 7

**†Corresponding Author:**

Clinton T. Rubin, Ph.D.

Department of Biomedical Engineering

Stony Brook University

Stony Brook, New York 11794-2580

Phone: (631) 632 1188

Fax: (631) 632 8577

E-mail: [clinton.rubin@sunysb.edu](mailto:clinton.rubin@sunysb.edu)

**Key Words:** *mesenchymal stem cells, bone, osteoblasts, osteoporosis, mechanical, loading, anabolic, therapeutics, adipogenesis, adiposity, adipocytes, fat, prevention, type 2 diabetes.*

## ABSTRACT

Mesenchymal stem cells (MSCs), a population of adult stem cells, are defined by their ability to self-renew and differentiate into the cells which form mesodermal tissues such as bone and fat. In young male C57BL/6J mice, 6w of extremely low magnitude mechanical signals (LMMS) increased the bone marrow stem cell population by 37% and the number of MSCs by 46% relative to sham controls. Concomitant with the increase in the number of stem cells, the differentiation potential of the MSCs was strongly biased towards osteoblastic over adipogenic differentiation, as reflected by Runx2 expression, a key transcription factor in osteoblastogenesis, upregulated in the bone marrow by 72%, while PPAR $\gamma$ , a gene central to adipogenesis, was downregulated by 27%. The ability of LMMS to influence MSC lineage determination was demonstrated in a mouse model of high fat diet induced obesity (DIO), where 14w of LMMS suppressed visceral adipose tissue formation in the torso by 28% while simultaneously increasing trabecular bone volume fraction in the tibia by 11%. The inability of LMMS to *reduce* fat volume in mice that were *already* obese indicates that the *prevention* of obesity in DIO was achieved primarily by mechanical influences on developmental pathways. Translating this to the clinic, a one year trial on young women with osteopenia (15-20y; n=48) showed that, relative to baseline, LMMS significantly increased trabecular bone density in the vertebrae and musculature around the spine, while keeping visceral fat at baseline levels, as compared to control subjects where bone density and muscle area failed to increase but the area of visceral fat rose significantly. Therapeutic targeting of stem cell proliferation and differentiation by mechanical signals indicates a promising strategy for tissue regenerative therapy, as well as the basis of a non-pharmacologic strategy to simultaneously prevent obesity and osteoporosis, diseases linked by a common precursor.

## INTRODUCTION

Bone marrow houses a diverse population of cells belonging to several lineages, including stem cells of both hematopoietic and mesenchymal origin. Pluripotent mesenchymal stem cells (MSCs) are considered ideal therapeutic targets in regenerative medicine, as they hold the capacity to differentiate into osteoblasts, adipocytes, fibroblasts, chondrocytes, and myocytes, and thus central to the formation of bone, fat, skin, ligament, tendon, cartilage and muscle. However, the pertinent environmental cues that regulate the lineage selection of MSCs remain largely unknown, making it difficult to harness this potential for application in the clinic.<sup>1-3</sup>

When the bone marrow stem cell population is driven to differentiate towards one cell fate, the establishment of another cell type is inherently suppressed. More specifically, MSCs express small amounts of both adipogenic and osteogenic factors, which cross regulate to retain the cell in an undifferentiated state.<sup>4</sup> When oncostatin, a member of the IL-6 family, is used to promote osteogenesis it simultaneously inhibits adipogenesis.<sup>5</sup> Conversely, anti-diabetic thiazolidinediones such as Rosiglitazone, a potent activator of PPAR $\gamma$ , promotes adipogenesis while suppressing osteogenesis.<sup>6-8</sup> Hyper-physiologic levels of tensile strain will increase proliferation of bone marrow cells,<sup>9</sup> and can down-regulate PPAR $\gamma$  in the local bone marrow, thus favoring osteoblastogenesis over adipogenesis.<sup>10</sup> These examples indicate an inversely coupled relationship of adipocytes and osteoblast differentiation, as dependent on fate decisions of their common precursor, the MSC.

The potential to harness MSCs as a means of treatment for injury and disease is dependent on an improved understanding of the means by which exogenous signals regulate their activity, and the ability of these stimuli to influence either/both proliferation and differentiation.<sup>11</sup> Pharmacologic enhancement of stem cell proliferation has recently been demonstrated *in vivo*,<sup>12</sup> while extremely low magnitude mechanical signals (LMMS) were shown to suppress adipogenesis in the growing animal without the use of drugs.<sup>13</sup> Utilizing a model of dietary induced obesity (DIO), the work presented here demonstrates that non-invasive

mechanical signals can markedly elevate the total number of stem cells in the marrow, and can bias their differentiation towards osteoblastogenesis, resulting in both an enhancement of bone density and the inhibition of visceral fat formation. A trial on young osteopenic women provides preliminary evidence that the therapeutic potential of low magnitude mechanical signals can be translated to the clinic, with a promotion of bone and muscle mass, and a concomitant suppression of visceral fat formation.

## **METHODS**

**Animal Model to Prevent Diet Induced Obesity.** All animal procedures were reviewed and approved by the Stony Brook University animal care and use committee. The overall experimental design consisted of two similar protocols, differing in the duration of treatment to assess mechanistic responses of cells to LMMS (6w of LMMS compared to control, n=8 per group) or to characterize the phenotypic effects (14w of LMMS compared to control). Two models of DIO were employed: 1. To examine the ability of LMMS to prevent obesity, a “Fat Diet” condition (n=12 each, LMMS and CON) was evaluated where LMMS and DIO were initiated simultaneously, and 2. To examine the ability of LMMS to reverse obesity, an “Obese” condition (n=8 each, LMMS and CON) was established, whereby LMMS treatment commenced 3 weeks after the induction of DIO, and compared to sham controls.

**Mechanical enhancement of stem cell proliferation and differentiation in DIO.** Beginning at 7w of age, C57BL/6J male mice were given free access to a high fat diet (45% kcal fat, # 58V8, Research Diet, Richmond, IN). The mice were randomized into two groups defined as LMMS (5d/w of 15min/d of a 90Hz, 0.2g mechanical signal, where 1.0g is earth’s gravitational field, or  $9.8\text{m/s}^2$ ), and placebo sham controls (CON). The LMMS protocol<sup>13</sup> provides low magnitude, high frequency mechanical signals by a vertically oscillating platform,<sup>14</sup> and generates strain levels in bone tissue of less than five microstrain, several orders of magnitude

below peak strains generated during strenuous activity.<sup>15</sup> Food consumption was monitored by weekly weighing of food.

**Status of MSC pool by flow cytometry.** Cellular and molecular changes in the bone marrow resulting from 6w LMMS (n=8 animals per group, CON or LMMS) were determined at sacrifice from bone marrow harvested from the right tibia and femur (animals at 13w of age). Red blood cells in the bone marrow aspirate were removed by room temperature incubation with Pharmlyse (BD Bioscience) for 15 mins. Single cell suspensions were prepared in 1% sodium azide in PBS, stained with the appropriate primary and (when indicated) secondary antibodies, and fixed at a final concentration of 1% formalin in PBS. Phycoerythrin (PE) conjugated rat anti-mouse Sca-1 antibody and isotype control were purchased from BD Pharmingen and used at 1:100. Rabbit anti-mouse Pref-1 antibody and FITC conjugated secondary antibody were purchased from Abcam (Cambridge, MA) and used at 1:100 dilutions. Flow cytometry data was collected using a Becton Dickinson FACScaliber flow cytometer (San Jose, CA).

**RNA extraction and real-time RT-PCR.** At sacrifice, the left tibia and femur were removed and marrow flushed into an RNAlater solution (Ambion, Foster City, CA). Total RNA was harvested from the bone marrow using a modified TRIs핀 protocol. Briefly, TRIzol reagent (Life Technologies, Gaithersburg, MD) was added to the total bone marrow cell suspension and the solution homogenized. Phases were separated with chloroform under centrifugation. RNA was precipitated via ethanol addition and applied directly to an RNeasy Total RNA isolation kit (Qiagen, Valencia, CA). DNA contamination was removed on column with RNase free DNase. Total RNA was quantified on a Nanodrop spectrophotometer and RNA integrity monitored by agarose electrophoresis. Expression levels of candidate genes was quantified using a real-time RT-PCR cycler (Lightcycler, Roche, IN) relative to the expression levels of samples spiked with

exogenous cDNA.<sup>16</sup> A “one-step” kit (Qiagen) was used to perform both the reverse transcription and amplification steps in one reaction tube.

**qRT-PCR with Content Defined 96 Gene Arrays.** PCR arrays were obtained from Bar Harbor Biotech (Bar Harbor, ME), with each well of a 96 well PCR plate containing gene specific primer pairs. The complete gene list for the osteoporosis array can be found at [www.bhbio.com](http://www.bhbio.com), and include genes that contribute to bone mineral density through bone resorption and formation, genes that have been linked to osteoporosis, as well as biomarkers and gene targets associated with therapeutic treatment of bone loss. cDNA samples were reversed transcribed (Message Sensor RT Kit, Ambion, Foster City, CA) from total RNA harvested from bone marrow cells and used as the template for each individual animal. Data were generated using an Applied Biosystems 7900HT real-time PCR machine, and analyzed by Bar Harbor Biotech.

**Body habitus established by *in vivo* microcomputed tomography ( CT)** Phenotypic effects of DIO, for both the “prevention” and “reversal” of obesity test conditions were defined after 12 and 14w of LMMS. At 12w, *in vivo*  $\mu$ CT scans were used to establish fat, lean, and bone volume of the torso (VivaCT 40, Scanco Medical, Bassersdorf, Switzerland). Scan data was collected at an isotropic voxel size of 76  $\mu$ m (45 kV, 133  $\mu$ A, 300-ms integration time), and analyzed from the base of the skull to the distal tibia for each animal. Threshold parameters were defined during analysis to segregate and quantify fat and bone volumes. Lean volume was defined as animal volume that is neither fat nor bone, and includes muscle and organ compartments. Detailed CT scanning protocol and analysis techniques are reported elsewhere.<sup>17, 18</sup>

**Bone phenotype established by *ex vivo* microcomputed tomography.** Trabecular bone morphology of the proximal region of the left tibia of each mouse was established by  $\mu$ CT at

12 $\mu$ m resolution ( $\mu$ CT 40, Scanco Medical, Bassersdorf, Switzerland). The metaphyseal region spanned 600  $\mu$ m, beginning 300 $\mu$ m distal to the growth plate. Bone volume fraction (BV/TV), connectivity density (Conn.D), trabecular number (Tb.N), trabecular thickness (Tb.Th), trabecular separation (Tb.Sp), and the structural model index (SMI) were determined.

**Serum and tissue biochemistry.** Blood collection was performed after overnight fast by cardiac puncture with the animal under deep anesthesia. Serum was harvested by centrifugation (14,000 rpm, 15 min, 4°C). Mice were euthanized by cervical dislocation, and the different tissues (i.e., epididymal fat pad and subcutaneous fat pads from the lower torso, liver, and heart) were excised, weighed, frozen in liquid nitrogen, and stored at -80°C. Total lipids from white adipose tissue (epididymal fat pad) and liver were extracted and purified based on a chloroform–methanol extraction. Total triglycerides (TG) and non-esterified free fatty acids (NEFA) were measured on serum (n=10 per group) and lipid extracts from adipose tissue (n=5 or 6 per group) and liver (n=10 per group) using enzymatic colorimetric kits (TG Kit from Sigma, Saint Louis, MO; and NEFA C from Wako Chemicals, Richmond, VA). ELISA assays were utilized to determine serum concentrations of leptin, adiponectin, resistin (all from Millipore, Chicago, IL), osteopontin (R&D Systems, Minneapolis, MN), and osteocalcin (Biomedical Technologies Inc, Stoughton, MA), using a sample size of n=10 per group.

**Clinical trial to examine inverse relationship of bone and fat formation.** A trial designed and conducted to evaluate if 12 months of LMMS could promote bone density in the spine and hip of women with low bone density was retrospectively evaluated to examine if changes in visceral fat volume were evident. All procedures were reviewed and approved by the Childrens Hospital of Los Angeles Committee on Research in Human Subjects. Forty-eight healthy young women (aged 15-20 years) were randomly assigned into either LMMS or CON groups (n=24 in each group). The LMMS group underwent brief (10 min requested), daily treatment

with LMMS (30 Hz signal @ 0.3g) for one year. Computed tomographic scans (CT) were performed at baseline and one year, with the same scanner (model CT-T 9800, General Electric Co., Milwaukee, WI), the same reference phantom for simultaneous calibration, and specially designed software for fat and muscle measurements. Identification of the abdominal site to be scanned was performed with a lateral scout view, followed by a cross-sectional image obtained from the midportion of the third lumbar vertebrae at 80 kVp, 70 milliamperes, and 2S.

Cancellous bone of the 1st, 2nd and 3rd lumbar vertebrae was established as measures of the tissue density of bone in milligrams per cubic centimeter ( $\text{mg}/\text{cm}^3$ ). Area of visceral fat ( $\text{cm}^2$ ) was defined at the mid-portion of the third lumbar vertebrae as the intra-abdominal adipose tissue surrounded by the rectus abdominus muscles, the external oblique muscles, the quadratus lumborum, the psoas muscles and the lumbar spine at the mid-portions of the third lumbar vertebrae, and consisted mainly of perirenal, pararenal, retroperitoneal and mesenteric fat. The average area of paraspinous musculature ( $\text{cm}^2$ ) was defined as the sums of the area of the erector spinae muscles, psoas major muscles and quadratus lumborum muscles at the mid-portion of the third lumbar vertebrae.<sup>19</sup> All analyses of bone density, and muscle and fat area were performed by an operator blinded as to subject enrollment.

**Statistical analyses.** All data are shown as mean  $\pm$  standard deviation, unless otherwise noted. To determine significant differences between LMMS and CON groups, two tailed t-tests (significance value set at 5%) were used throughout. Animal outliers were determined based on animal weight at baseline (before the start of any treatment) as animals falling outside of two standard deviations from the total population, or in each respective group at the end of 6 or 14 weeks LMMS (or sham CON) by failure of the Weisberg one-tailed t-test ( $\alpha = 0.01$ ), regarded as an objective tool for showing consistency within small data sets.<sup>20</sup> No outliers were identified in the 6w CON and LMMS groups. Two outliers per group (CON and LMMS) were identified in the Fat Diet model (14w LMMS study) and removed. Data from these animals were not included in



any analyses, resulting in a sample size of n=10 per group for all data, unless otherwise noted. No outliers were identified in the 14w Obese model (n=8). Data presented from the human trial are based on the Intention-To-Treat data set (all subjects included in the evaluation). Changes in visceral fat volume were compared between LMMS and CON subjects using a one tailed t-test.

## RESULTS

**Bone marrow stem cell population is promoted by LMMS.** Flow cytometric measurements using antibodies against Stem Cell Antigen-1 (Sca-1) indicated that in animals in the “prevention” DIO group, 6w of LMMS treatment significantly increased the overall stem cell population relative to controls, as defined by cells expressing Sca-1. Analysis focused on the primitive population of cells with low forward (FSC) and side scatter (SSC), indicating the highest Sca-1 staining for all cell populations. Cells in this region demonstrated a 37.2% (p=0.028) increase in LMMS stem cell numbers relative to sham CON animals. Mesenchymal stem cells as represented by cells positive for Sca-1 and Preadipocyte Factor-1 (Pref-1),<sup>1</sup> represented a much smaller percentage of the total cells. Identified in this manner, in addition to the increase in the overall stem cell component, LMMS treated animals had a 46.1% (p=0.022) increase in mesenchymal stem cells relative to CON (Fig 1).

**LMMS biases marrow environment and lineage commitment towards osteogenesis.** After six weeks, cells expressing only the Pref-1 label, considered committed preadipocytes, were elevated by 18.5% (p=0.25) in LMMS treated animals relative to CON (Fig 2). Osteoprogenitor cells in the bone marrow population, identified as Sca-1 positive with high FSC and SSC,<sup>21</sup> were 29.9% greater (p=0.23) greater when subject to LMMS. This trend indicating that differentiation in the marrow space of LMMS animals had shifted towards osteogenesis was confirmed by gene expression data, which demonstrated that transcription of Runx2 in total bone marrow

isolated from LMMS animals was upregulated 72.5% ( $p=0.021$ ) relative to CON. In these same LMMS animals, expression of PPAR $\gamma$  was downregulated by 26.9% ( $p=0.042$ ) relative to CON (Fig 3).

Gene expression data on bone marrow samples were also tested on a 96 gene “osteoporosis” array, which included genes that contribute to bone mineral density through bone resorption and formation, and genes that have been linked to osteoporosis through association studies. Samples for both CON and LMMS groups expressed 83 of the 94 genes present on the array. qRT-PCR arrays reported decreases in genes such as Pon1 (paraoxonase-1), is known to be associated with high density lipoproteins (-137%,  $p = 0.26$ ), and sclerostin (-258%,  $p=0.042$ ), which antagonizes bone formation by acting on Wnt signaling.<sup>22</sup> Genes such as estrogen related receptor (Esrra; +107%,  $p=0.018$ ) and Pomc-1 (pro-opiomelanocortin, +68%,  $p=0.055$ ) were up-regulated by LMMS.

**LMMS enhancement of bone quantity and quality.** The ability of LMMS induced changes in proliferation and differentiation of MSCs to elicit phenotypic changes in the skeleton was first measured at 12w by *in vivo*  $\mu$ CT scanning of the whole mouse (neck to distal tibia). Animals subject to LMMS showed a 7.3% ( $p=0.055$ ) increase in bone volume fraction of the axial and appendicular skeleton (BV/TV) over sham CON. Post-sacrifice, 12  $\mu$ m resolution  $\mu$ CT scans of the isolated proximal tibia of the LMMS animals showed 11.1% ( $p=0.024$ ) greater bone volume fraction than CON (Fig 4). The micro architectural properties were also enhanced in LMMS as compared to CON, as evidenced by 23.7% greater connectivity density ( $p=0.037$ ), 10.4% higher trabecular number ( $p=0.022$ ), 11.1% smaller separation of trabeculae ( $p=0.017$ ) and a 4.9% lower structural model index (SMI,  $p=0.021$ ; Table 1).

**Prevention of obesity by LMMS:** At 12w, neither body mass gains nor the average weekly food intake differed significantly between the LMMS or CON groups (Table 2). At this point,

(19w of age), CON weighed  $32.9\text{g} \pm 4.2\text{g}$ , while LMMS mice were 6.8% lighter at  $30.7\text{g} \pm 2.1\text{g}$  ( $p=0.15$ ). CON were 15.0% heavier than mice of the same strain, gender and age that were fed a regular chow diet,<sup>13</sup> and increase in body mass due to high fat feeding was comparable to previously reported values.<sup>23</sup> Adipose volume from the abdominal region (defined as the area encompassing the lumbar spine) was segregated as either subcutaneous or visceral adipose tissue (SAT or VAT, respectively). LMMS animals had 28.5% ( $p=0.021$ ) less VAT by volume, and 19.0% ( $p=0.016$ ) less SAT by calculated volume. Weights of epididymal fat pads harvested at sacrifice (14w) correlated strongly with fat volume data obtained by CT. The epididymal fat pad weight was 24.5% ( $p=0.032$ ) less in LMMS than CON, while the subcutaneous fat pad at the lower back region was 26.1% ( $p=0.018$ ) lower in LMMS (Table 2).

**LMMS prevents increased biochemical indices of obesity.** Triglycerides (TG) and non-esterified free fatty acids (NEFA) measured in plasma, epididymal adipose tissue, and liver were all lower in LMMS as compared to CON (Table 3). Liver TG levels decreased by 25.6% ( $p=0.19$ ) in LMMS animals, paralleled by a 33.0% ( $p=0.022$ ) decrease in NEFA levels. Linear regressions of adipose and liver TG and NEFA values to  $\mu\text{CT}$  visceral volume (VAT) demonstrated strong positive correlations for CON animals, with  $R^2 = 0.96$  ( $p=0.002$ ) for adipose TG,  $R^2 = 0.85$  ( $p=0.027$ ) for adipose NEFA,  $R^2 = 0.64$  ( $p=0.006$ ) for liver TG and  $R^2 = 0.80$  ( $p=0.003$ ) for liver NEFA (Fig 5). LMMS resulted in weaker correlations between all TG and NEFA levels to increases in VAT.

At sacrifice, fasting serum levels of adipokines were lower in LMMS as compared to CON. Circulating levels of leptin were 35.3% ( $p=0.05$ ) lower, adiponectin was 21.8% ( $p=0.009$ ) lower, and resistin was 15.8% lower ( $p=0.26$ ) than CON (Table 3). Circulating serum osteopontin (-7.5%,  $p=0.41$ ) and osteocalcin (-14.6%,  $p=0.22$ ) levels were not significantly affected by the mechanical signals.

**LMMS fails to reduce existing adiposity.** In the “reversal” model of obesity, 4w old animals were started on a high fat diet for 3w prior to beginning the LMMS protocol at 7w of age. These “obese” animals were on average 3.7 grams heavier ( $p < 0.001$ ) than chow fed regular diet animals (baseline) at the start of the protocol. The early-adolescent obesity in these mice translated to adulthood, such that by the end of the 12w protocol, they weighed 21% more than the CON animals who began the fat diet at 7w of age ( $p < 0.001$ ). In stark contrast to the “prevention” animals, where LMMS realized a 22.2% ( $p=0.03$ ) lower overall adipose volume relative to CON (distal tibia to the base of the skull), no differences were seen for fat (-1.1%,  $p=0.92$ ), lean (+1.3%,  $p=0.85$ ), or bone volume (-0.2%,  $p=0.94$ ) between LMMS and sham control groups after 12w of LMMS for these already obese mice (Fig 6).

**LMMS promotes bone and muscle formation while suppressing visceral fat formation in humans.** To determine whether the capacity of LMMS to suppress adiposity and increase osteogenesis in mice can translate to the human, young women with low bone density were subject to daily exposure to LMMS for 12 months. The study cohort ranged from 15-20 years old, and represented an osteopenic cohort. Detailed descriptions of this study population are provided elsewhere.<sup>19</sup> Over the course of one year, women ( $n=24$ ) in the CON group had no significant change in cancellous bone density of the spine relative to baseline ( $0.1\text{mg}/\text{cm}^3 \pm \text{s.e.}1.5$ ;  $p=0.93$ , Fig 7), as compared to a  $3.8\text{mg}/\text{cm}^3 \pm 1.6$  increase in the spine of the LMMS treated cohort ( $p=0.03$ ). Further, the average area of paraspinous muscle at the mid-portion of the third lumbar vertebrae, which failed to change from baseline in CON ( $1.2\text{cm}^2 \pm 1.9$ ;  $p=0.52$ ), was sharply elevated in the LMMS women ( $10.1\text{cm}^2 \pm 2.5$ ;  $p<0.001$ ). The area of visceral fat measured at the lumbrosacral region of CON subjects increased significantly from baseline by  $5.6\text{cm}^2 \pm 2.4$  ( $p=0.015$ ). In contrast, the area of visceral fat measured in LMMS subjects increased by only  $1.8\text{cm}^2 \pm 2.3$ , which was not significantly different from baseline ( $p=0.22$ ).

## DISCUSSION

The experiments reported here indicate that extremely low magnitude mechanical signals, well below those generated during locomotion, can promote the number of stem cells residing in the marrow. Further, these subtle mechanical signals biased the differentiation of the MSC cohort towards osteoblastogenesis over adipogenesis, such that obesity was prevented while the formation of bone was simultaneously promoted. These data provide support for the growing body of evidence of an inversely coupled relationship between pre-osteoblasts and pre-adipocytes in the marrow cavity, and osteogenesis and adipogenesis overall.<sup>24</sup> Translating the therapeutic potential of controlling stem cell proliferation and differentiation to a group of young osteopenic women, these low magnitude mechanical signals promoted bone and muscle mass, simultaneously suppressing the accumulation of visceral fat in the treated group, while controls failed to gain either bone or muscle, but showed a significant increase in visceral fat.

Sca-1 is an antigen previously associated with hematopoietic cells, but more recently cells expressing Sca-1 have been demonstrated to exhibit adipogenic, chondrogenic and osteogenic potential.<sup>25</sup> Sca-1 was used to give a general indication of the status of the bone marrow cell population, representing both hematopoietic and mesenchymal stem cells as the marker does not distinguish between the two cell types. The relative increase in the overall bone marrow stem cell population induced by LMMS reflected an enhancement of stem cells of both hematopoietic and mesenchymal lineages. The method utilized for bone marrow harvesting (flushing of bones) does not remove the significant portion (33%) of hematopoietic stem cells (HSCs) that resides in proximity to the endosteal surface of the bone,<sup>26</sup> and thus the influence of LMMS on HSC's is likely underestimated in this model. Cells expressing both Sca-1 and Pref-1 are more specific in identifying mesenchymal stem cells, and while these cells occur less frequently, this population demonstrated a larger increase to LMMS than that measured in the overall stem cell population. In all, these data indicate that the stem cell pool has been positively influenced by mechanical signals, resulting in an increase in total number of cells.

At the molecular level, LMMS induced a clear shift in the biological balance of key osteogenic and adipogenic factors, including a marked increase in the expression levels of Runx2, and a significant decrease in the level of PPAR $\gamma$ . Together, this change in balance would conspire to push stem cells in the undifferentiated state preferentially towards the formation of bone and away from fat.<sup>24</sup> PPAR $\gamma$  activation has been shown to change marrow structure and function by decreasing the multipotential character of mesenchymal stem cells.<sup>7</sup> Reduced levels of PPAR $\gamma$  are known to be permissive to osteoblastogenesis and lead to higher trabecular bone volume,<sup>27</sup> by promoting the osteoblastic lineage decision of MSCs.<sup>28</sup> Data from the PCR arrays highlights that – despite the marked changes in bone and fat phenotype, relatively few genes have changed expression in response to the LMMS, emphasizing that the adaptive response of the organism is quite subtle, particularly when considered relative to the robust, complex transcriptional activity related to repair.<sup>29</sup> That said, those genes that were upregulated (i.e. Esrra, Pomc1) have been shown to be osteogenic and/or protective of obesity, while those genes that were down-regulated (ie. sclerostin, Pon1) are related to osteoclast activity and lipogenesis. While the full mechanistic pathway by which LMMS is sensed and transduced in the bone marrow environment is as of yet undetermined, the data indicate that genes implicated in signaling cascades controlling bone development are up-regulated, and those influencing adipose development are down-regulated, all by a barely perceptible physical signal transduced to the marrow.

While not statistically significant, the increased percentage of cells in the osteoprogenitor and preadipocyte populations in bone marrow from the LMMS animals showed trends which support a conclusion that lineage selection of cells has been altered by the mechanical signal. There is evidence suggesting that preadipocytes, through expression of the plasma membrane protein Pref-1, are responsive to differentiation signals from the extracellular environment,<sup>30</sup> with Pref-1 expression actually being *inhibitory* of adipogenesis and terminal adipocyte differentiation.<sup>31</sup> The ultimate fate of marrow preadipocytes and their ability to migrate to other

adipose tissue depots has not been definitively addressed and ultimately may highlight the inherent difficulty in harnessing stem cell plasticity as a therapeutic endpoint.<sup>32, 33</sup>

While the influence of LMMS has been evaluated in bone marrow derived stem cells, it is important to recognize that the mechanical signal is delivered systemically and thus does not preclude other cell populations from being subject to the stimulus. Indeed, we do not categorically conclude that the phenotypic changes measured in fat and bone are exclusively the result of regulating the bone marrow stem cell population, and changes in the visceral fat compartment, for one, may derive through the influence of other stem cell populations. What is apparent, however, is that LMMS increases the size of the precursor pool, and biases them away from adipogenesis and towards higher order connective tissues. We believe these data support a conclusion that the mechanical biasing of MSC lineage selection towards osteoblastogenesis inherently suppresses adipogenesis because a given stem cell can make only a “single pathway” commitment. Indeed, even though adipose tissue mass was more than twenty percent greater in the controls relative to the LMMS animals, differences in animal weights were not significant, as the reduced fat mass of the LMMS animals was to a degree, compensated by an increase in bone mass, further emphasizing the binary nature of decision making in the differentiation process.

While these data indicate a critical role of development in obesity, they of course do not preclude an influence on the overall metabolic state of the animal, as increased adiposity inherently will alter the systemic physiology of the organism by changing the endocrine and metabolic state of the fat tissue.<sup>34</sup> The marked disparities of fat mass measured between control and LMMS groups will inevitably influence their relative susceptibility to the metabolic consequences of obesity, particularly considering the capacity of LMMS to suppress visceral adipose tissue (VAT). VAT is an important risk factor to metabolic complications which afflict the obese, with adiposity positively correlating with fasting plasma insulin, triglyceride (TG), low-density lipoprotein (LDL) and apolipoprotein B (apo B) levels, as well as the cholesterol

(CHOL)/high-density lipoprotein (HDL)-CHOL ratio.<sup>35</sup> Increased abdominal adiposity is also known to be a significant risk factor for type 2 diabetes.<sup>36</sup> Control animals presented with these same positive correlations of TG and NEFA levels in adipose tissue and the liver to visceral adipose accumulation, while adipose gains in LMMS treated animals did not translate into proportional increases, suggesting that suppression of adipogenesis and/or adiposity inhibited the risk of associated disease sequelae.

Serum levels of osteopontin were measured to assay systemic changes in bone tissue, as osteopontin is secreted by osteoblasts and acts to activate osteoclasts in the normal process of bone remodeling. Additionally, osteopontin has been reported as a potent constraining factor on hematopoietic stem cell proliferation.<sup>37</sup> That osteopontin is unaffected by LMMS treatment highlights the general promotion of stem cell proliferation (HSC and MSC), but the specificity of the proposed mechanism to MSC differentiation as biasing the formation of osteoprogenitors did not examine if osteoclasts, which derive from HSCs, were activated. Circulating levels of the key adipokines leptin, adiponectin and resistin are known to be elevated under conditions of DIO, as these molecules are secreted by white adipose tissue.<sup>23, 38</sup> These molecules each exhibit pleiotropic effects, with implications for inflammatory and immune responses.<sup>39</sup> In light of the similar food intake between groups, the markedly reduced levels of circulating adipokines in LMMS animals may best reflect the reduced adipose burden in these mice.

In evaluating the ability of LMMS to prevent obesity, these data clearly indicate that these mechanical signals were effective at the molecular, cellular and tissue level, as indicated by a distinct bias towards osteogenesis after 6w, translating at 12 and 14w into clear phenotypic differences in bone and fat volume. In contrast, mice allowed to become obese (3w of a high fat diet) prior to LMMS stimulation indicated not only the inability of these mechanical signals to reverse obesity in animals that were already fat, it failed to influence their bone mass, despite receiving the same mechanical signal as the “prevention” group. This could either mean that the stem cell population in the “pre-obese” mice was already committed towards adipogenesis



by the time the mechanical signals were introduced, or that the adipogenic environment catalyzed by a high fat diet supersedes the ability of other exogenous signals to drive MSCs towards alternative lineages. Certainly, the inability to coax adipose tissue away from the obese animal emphasizes the starkly different challenges of a developmental strategy to prevent obesity versus the metabolic realities of reversing it. A similar scenario may well be evident in prevention versus the reversal of age-related bone loss, as the deterioration of the marrow based stem cell population which parallels aging may undermine the ability of any intervention to harness the potential of stem cells to treat disease.<sup>40</sup>

Aging animals demonstrate a significant reduction in their stem cell population and their regenerative capacity,<sup>41</sup> while simultaneously predisposing this environment towards adipogenesis in the remaining MSCs.<sup>42</sup> Extending this “aging” related deterioration to disuse, inactivity and microgravity markedly reduce osteoblastogenesis in the MSC pool,<sup>43</sup> while the actual number of osteoprogenitor cells is also severely compromised.<sup>44</sup> Thus, both age and activity are determinants of the viability of the stem cell population, and independently or together may conspire towards a reduced regenerative capacity. This deterioration can be somewhat mitigated by replenishment of the bone marrow stem cell population, either directly or via exposure to a “young” environment, showing promise as an intervention to restore musculoskeletal health.<sup>45, 46</sup> When considering this in the context of the data presented here in osteopenic women, where LMMS increased bone and muscle mass while simultaneously suppressing visceral adiposity, suggests that susceptibility to diseases such as obesity and osteoporosis may be more closely coupled than previously thought, due – potentially - to a failure to drive stem cells towards the “right” fate.

It has been estimated that 80% of obese adolescents develop into obese adults,<sup>47</sup> contributing to the conclusion by the American Heart Association that primary prevention is the key to constraining the societal impact,<sup>48</sup> as treatments available to the obese are limited. The differential response to LMMS in the two animal models presented here further highlights this

disparity, in that prevention of obesity via developmental control was achievable, but that reversal of an obese state, once cell fate had been pre-determined, was not realized. Rather than a metabolic pathway, these data indicate a developmentally mediated mechanism by which the suppression of fat and the enhancement of bone are coupled, linked to mechanical influences on stem cell populations. Indeed, the mechanically mediated increase in the number of progenitor cells, taken together with the ability of these mechanical signals to drive commitment choices, indicates a viable means to enhance an organism's regenerative capacity and reduce susceptibility to disease, achieved by exploiting stem cell sensitivity to physical signals.

## **ACKNOWLEDGEMENTS**

We thank S. Lublinsky, E. Ozcivici, B. Adler, and J. Pangilinan for help with animal imaging and tissue processing. Assistance from the lab of Dr. M. Hadjiargyrou, and the Stony Brook University Medical Center Flow Cytometry Facility is gratefully acknowledged. This work was supported by National Institutes of Health Grants AR 43498, AR 45433, and DK33823; National Aeronautics and Space Administration Grant NAG 9-1499; The Goldman Foundation; and a W. H. Coulter Translational Research Award.

**COMPETING INTERESTS STATEMENT:** C.T.R. is a founder of and consultant for Juvent Medical, Inc. C.T.R., S.J., and J.E.P. have submitted a provisional patent to the U.S. Patent and Trademark Office regarding the method and application of the technology.

**Table 1.** Micro-architectural parameters of trabecular bone in DIO animals measured at 14w (mean  $\pm$  s.d., n=10 in each group) demonstrate the enhanced structural quality of bone in the proximal tibia of LMMS treated animals as compared to controls.

	<b>CON</b>	<b>LMMS</b>	<b>% diff</b>	<b>p-value</b>
<b>Conn.D (1/mm<sup>3</sup>)</b>	105.3 $\pm$ 34.2	130.3 $\pm$ 28.9	<b>23.7</b>	<b>0.037</b>
<b>Tb.N (1/mm)</b>	3.06 $\pm$ 0.45	3.38 $\pm$ 0.37	<b>10.4</b>	<b>0.022</b>
<b>Tb.Th (mm)</b>	0.029 $\pm$ 0.001	0.030 $\pm$ 0.001	1.0	0.398
<b>Tb.Sp (mm)</b>	0.304 $\pm$ 0.046	0.270 $\pm$ 0.035	<b>-11.1</b>	<b>0.017</b>
<b>SMI</b>	2.93 $\pm$ 0.22	2.78 $\pm$ 0.14	<b>-4.9</b>	<b>0.021</b>

**Table 2:** Despite similar body mass and weekly food consumption, phenotypic parameters of the DIO animals after 12w of LMMS or at sacrifice (14w, mean  $\pm$  s.d., n=10 in each group) demonstrate a leaner body habitus as compared to CON, as the adipose burden (visceral and subcutaneous fat) is significantly lower in the mechanically stimulated animals.

	<b>CON</b>	<b>LMMS</b>	<b>% diff</b>	<b>p-value</b>
<b>Animal Weight at 12 weeks (grams)</b>	32.9 $\pm$ 4.12	30.7 $\pm$ 2.74	-6.8	0.152
<b>Weekly Food Consumption (grams)</b>	18.9 $\pm$ 1.57	18.5 $\pm$ 1.47	-2.5	0.406
<b>Visceral Adipose Tissue (VAT, cm<sup>3</sup>)</b>	2.3 $\pm$ 0.72	1.6 $\pm$ 0.34	<b>-28.5</b>	<b>0.021</b>
<b>Subcutaneous Adipose Tissue (SAT, cm<sup>3</sup>)</b>	0.84 $\pm$ 0.16	0.68 $\pm$ 0.08	<b>-19.0</b>	<b>0.016</b>
<b>Epididymal Fat Pad (grams)</b>	1.85 $\pm$ 0.52	1.40 $\pm$ 0.32	<b>-24.5</b>	<b>0.032</b>
<b>Subcutaneous Fat Pad (grams)</b>	0.67 $\pm$ 0.17	0.50 $\pm$ 0.12	<b>-26.1</b>	<b>0.018</b>
<b>Liver (grams)</b>	0.99 $\pm$ 0.16	0.94 $\pm$ 0.07	-4.9	0.399

**Table 3:** Biochemical parameters of the DIO animals (mean  $\pm$  s.d., n=10 in each group, unless otherwise noted) highlight lower level of TG, NEFA, and circulating adipokines following 14w in those subject to LMMS, as compared to controls.

	CON	LMMS	% diff	p-value
<b>TG Liver (total mg)</b>	31.8 $\pm$ 14.3	23.6 $\pm$ 12.7	-25.6	0.195
<b>NEFA Liver (total mol)</b>	7.5 $\pm$ 2.7	5.0 $\pm$ 1.5	<b>-33.0</b>	<b>0.022</b>
<b>TG Adipose (total mg)</b>	91.6 $\pm$ 34.6 (n=5)	72.9 $\pm$ 18.1 (n=6)	-20.4	0.321
<b>NEFA Adipose (total mmol)</b>	18.1 $\pm$ 5.8 (n=5)	15.3 $\pm$ 2.4 (n=6)	-15.8	0.345
<b>TG Serum (mg/dl)</b>	46.2 $\pm$ 17.0	47.0 $\pm$ 18.4	1.6	0.928
<b>NEFA Serum (mmol/l)</b>	0.68 $\pm$ 0.10	0.64 $\pm$ 0.14	-5.3	0.526
<b>Leptin Serum (ng/mL)</b>	15.9 $\pm$ 7.2	10.1 $\pm$ 4.7	<b>-37.6</b>	<b>0.049</b>
<b>Resistin Serum (ng/mL)</b>	4.3 $\pm$ 1.2	3.6 $\pm$ 1.0	-15.8	0.200
<b>Adiponectin Serum (<math>\mu</math>g/mL)</b>	9.2 $\pm$ 1.7	7.0 $\pm$ 1.4	<b>-23.5</b>	<b>&lt;0.01</b>
<b>Osteopontin Serum (ng/mL)</b>	197.8 $\pm$ 22.8	183.0 $\pm$ 39.6	-7.5	0.409
<b>Osteocalcin Serum (ng/mL)</b>	55.7 $\pm$ 17.2	47.6 $\pm$ 7.8	-14.6	0.218

**Figure 1.** As compared to Control DIO animals (A), mechanical signals increase the number, and influence the distribution, of stem cells in the bone marrow of LMMS animals (B). Representative dot plots from flow cytometry experiments indicate the ability of LMMS to increase the number of stem cells in general (Sca-1 single positive, upper quadrants), and MSCs specifically (both Sca-1 and Pref-1 positive, upper right quadrant). The actual increase in total stem cell number was calculated as percent positive cells per total cells for the cell fraction showing highest intensity staining (C). The ability of LMMS to specifically enhance MSC proliferation is even greater (D).

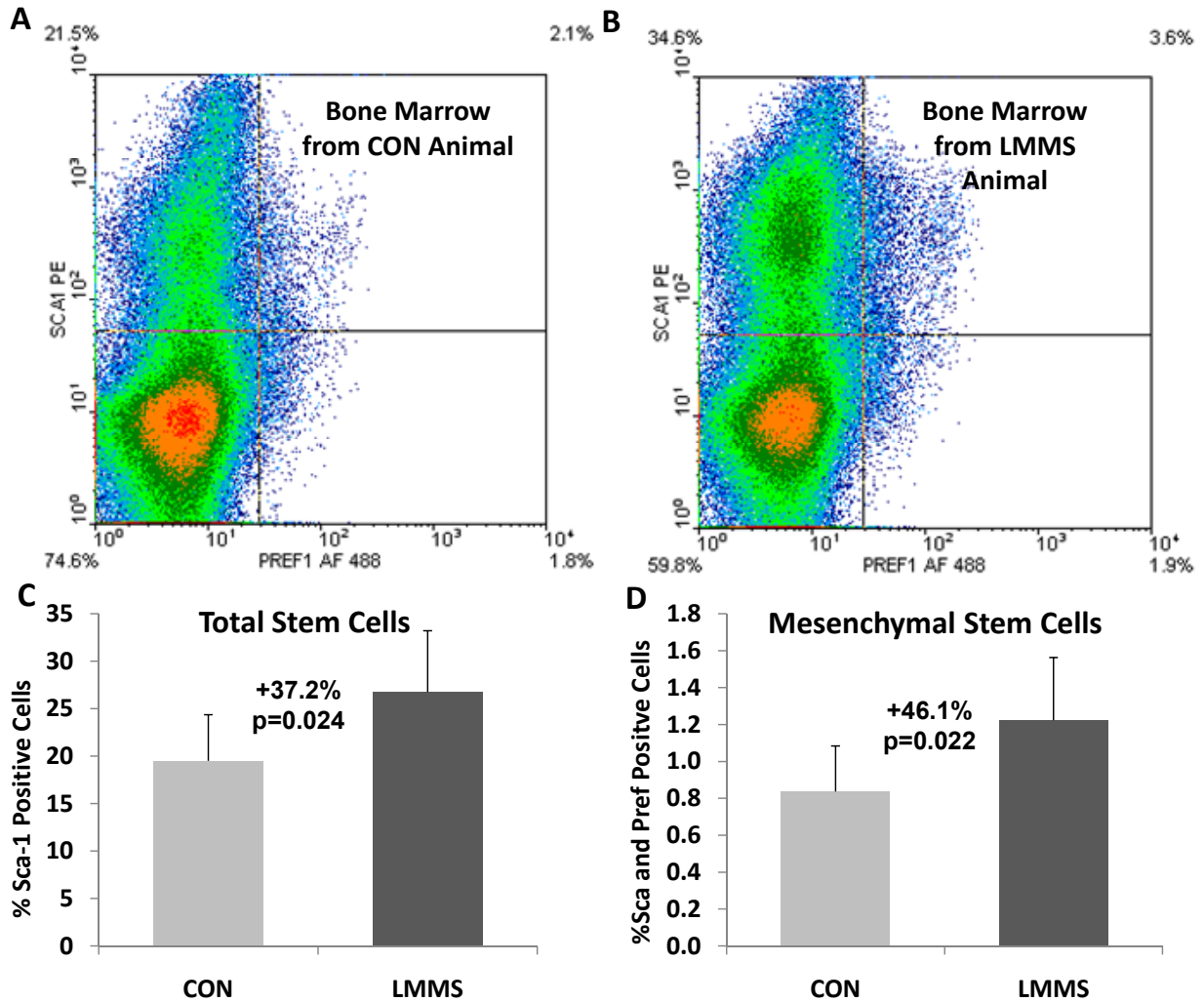


**Figure 2.** LMMS influences on stem cells of DIO animals was focused on the distinct cell populations identified in flow cytometry (A), with stem cells being identified as low forward (FSC) and side (SSC) scatter. Osteoprogenitor cells were identified as Sca-1(+) cells, residing in the region highlighted as high FSC and SSC, and were 29.9% (p=0.23) more abundant in the bone marrow of LMMS treated animals (B). The preadipocyte population, identified as Pref-1 (+), Sca-1 (-), demonstrated a trend (+18.5%; p=0.25) towards an increase in LMMS relative to CON animals (C).

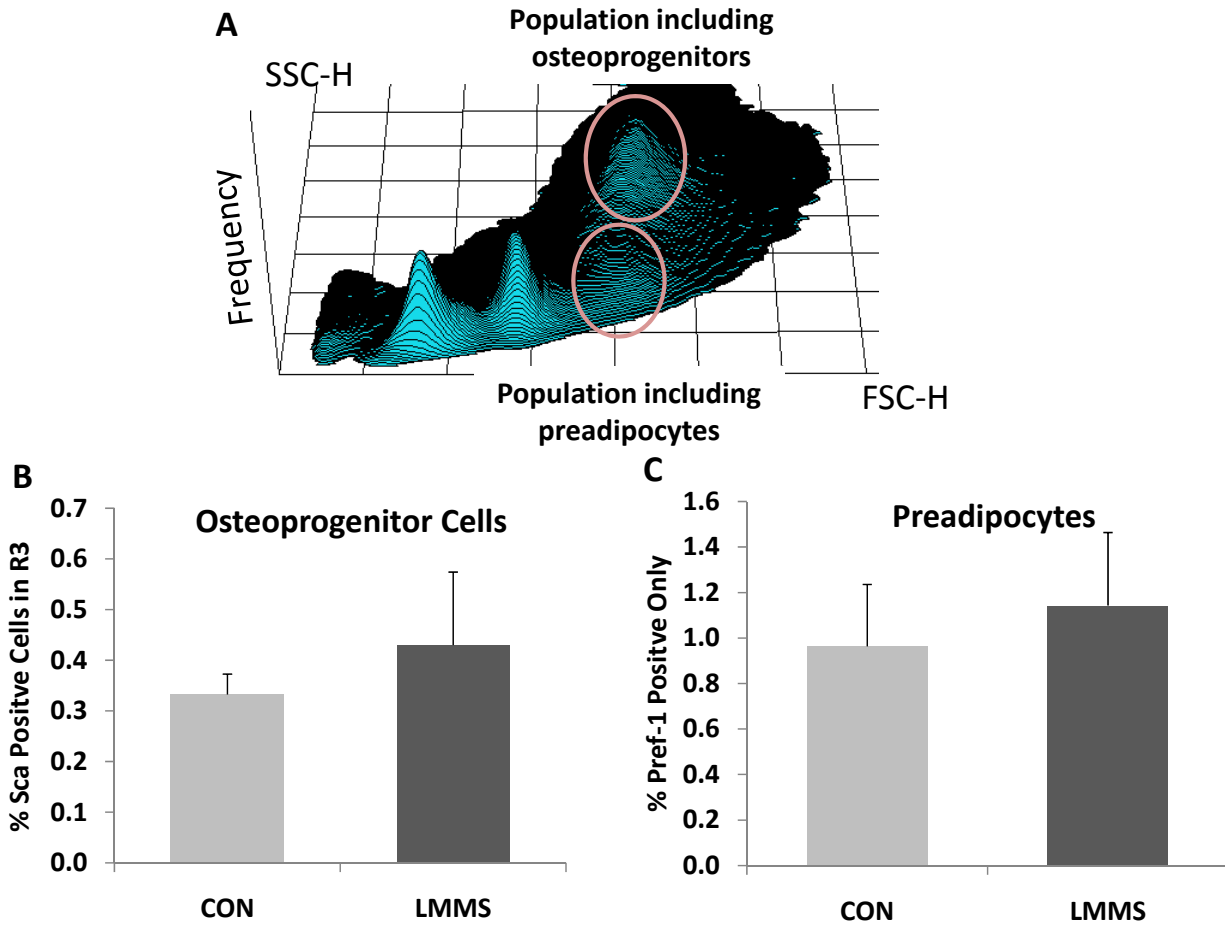




**Figure 3.** LMMS shifts the bone marrow environment of the DIO animals towards osteogenesis and away from adipogenesis. Real Time RT-PCR analysis of bone marrow samples harvested from animals subject to 6 weeks LMMS treatment, and compared to sham control, indicated a significant upregulation of the osteogenic gene Runx2 (A) and downregulation of the adipogenic gene PPAR $\gamma$  (B).

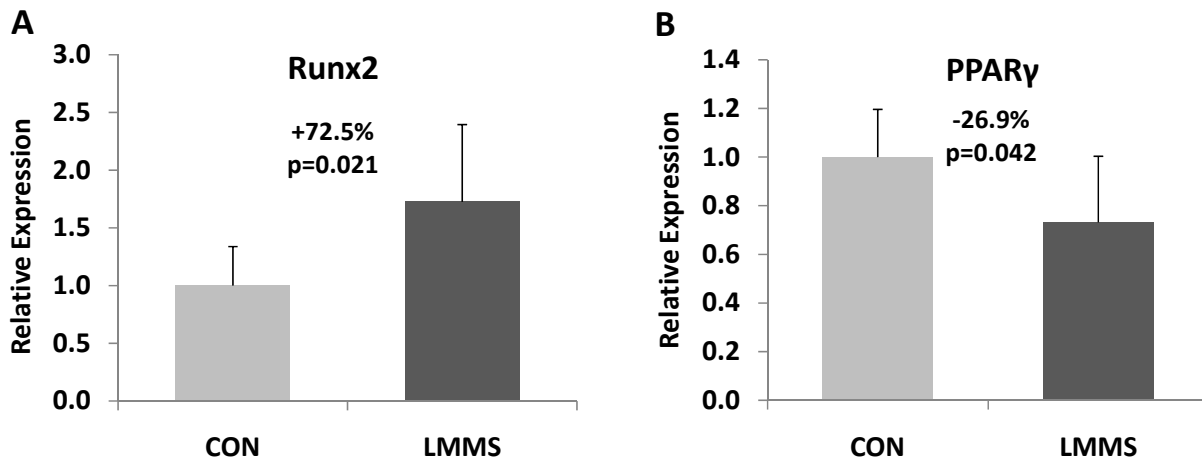


**Figure 4.** Bone volume fraction, as measured *in vivo* by low resolution  $\mu$ CT, indicated that LMMS increased bone volume fraction across the entire torso of the DIO animals (A). Post-sacrifice, high resolution CT of the proximal tibia indicated a significant increase in trabecular bone density (B). As compared to the trabecular compartment of control DIO animals (C), representative  $\mu$ CT reconstructions at the proximal tibia indicate the enhanced morphological properties of DIO animals subject to LMMS (D).

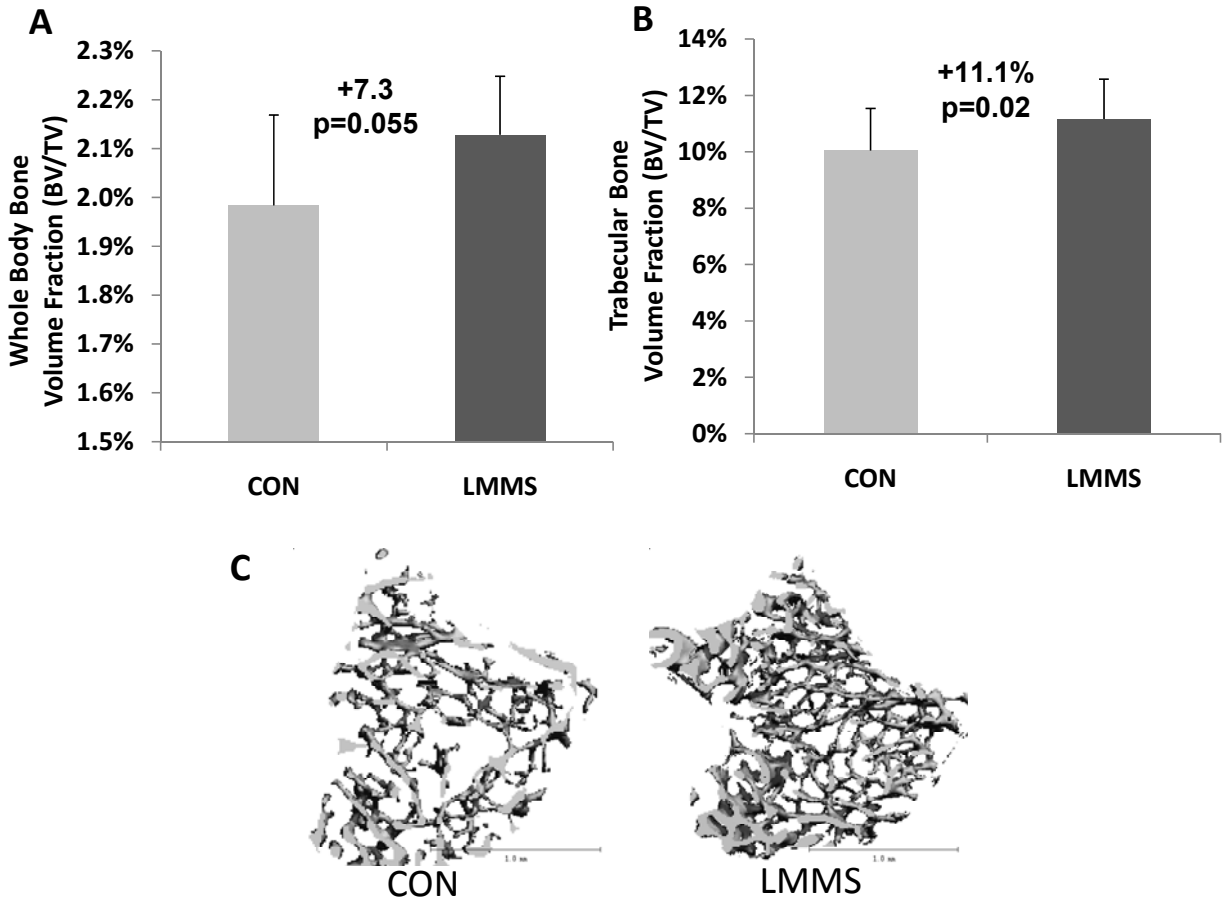


**Figure 5.** *In vivo*  $\mu$ CT images used to discriminate visceral and subcutaneous adiposity in the abdominal region of a CON and LMMS DIO animal (A; same scale). Visceral fat is shown in red, subcutaneous fat in gray (A). Linear regressions of calculated visceral adipose tissue (VAT) volume against adipose and liver biochemistry values demonstrated strong positive correlations in CON, and weak correlations in LMMS, as well as generally lower levels for all biochemical values in LMMS animals. N=6 for adipose (B), N=10 for liver (C,D). Regressions for adipose TG ( $p=0.002$ ), adipose NEFA ( $p=0.03$ ), liver TG ( $p=0.006$ ) and liver NEFA ( $p=0.003$ ) were significant for CON animals, but only liver NEFA ( $p=0.02$ ) was significant for LMMS. Overall, LMMS mice exhibited lower, non-significant correlations in liver TG ( $p=0.06$ ), adipose TG ( $p=0.19$ ), and adipose NEFA ( $p=0.37$ ) to increases in visceral adiposity. CON =  $\circ$ , LMMS =  $\blacksquare$

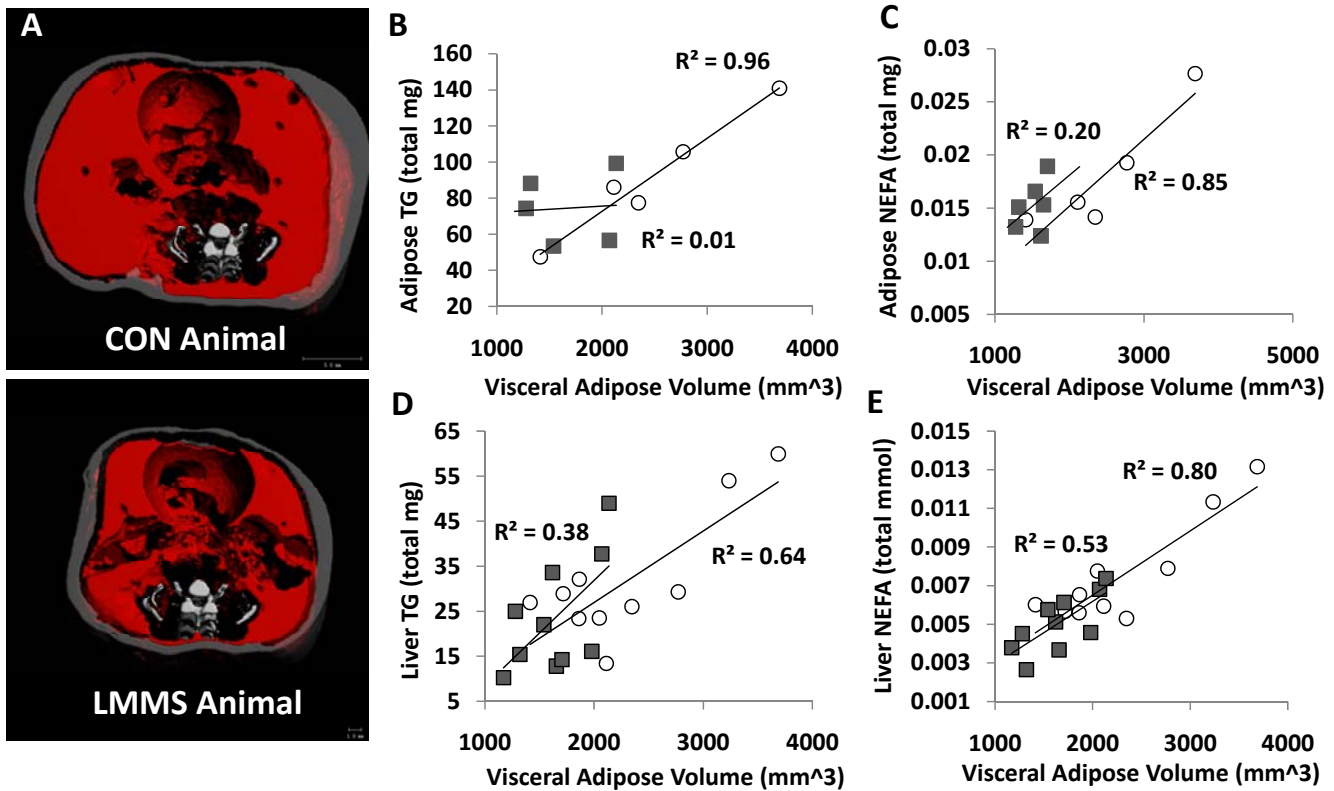


**Figure 6.** LMMS prevention of the obese phenotype in DIO animals was achieved to a degree by stem cells preferentially diverting from an adipogenic lineage. Reconstructed *in vivo*  $\mu$ CT images of total body fat (red; A) indicate that following 12w, animals which began LMMS at the time that the high fat diet was introduced exhibited 22.2% less fat volume as compared to control. In contrast, animals allowed a high fat diet for 3w prior to LMMS failed to demonstrate any reduction of fat volume or promotion of bone (B). Shown as a relative percentage of fat to total animal volume, LMMS reduced the percent animal adiposity by 13.5% ( $p=0.017$ ), while the lack of a response in the already obese animals reinforced a conclusion that the mechanical signal works primarily at the stem cell development level, as existing fat was not metabolized by LMMS stimulation.

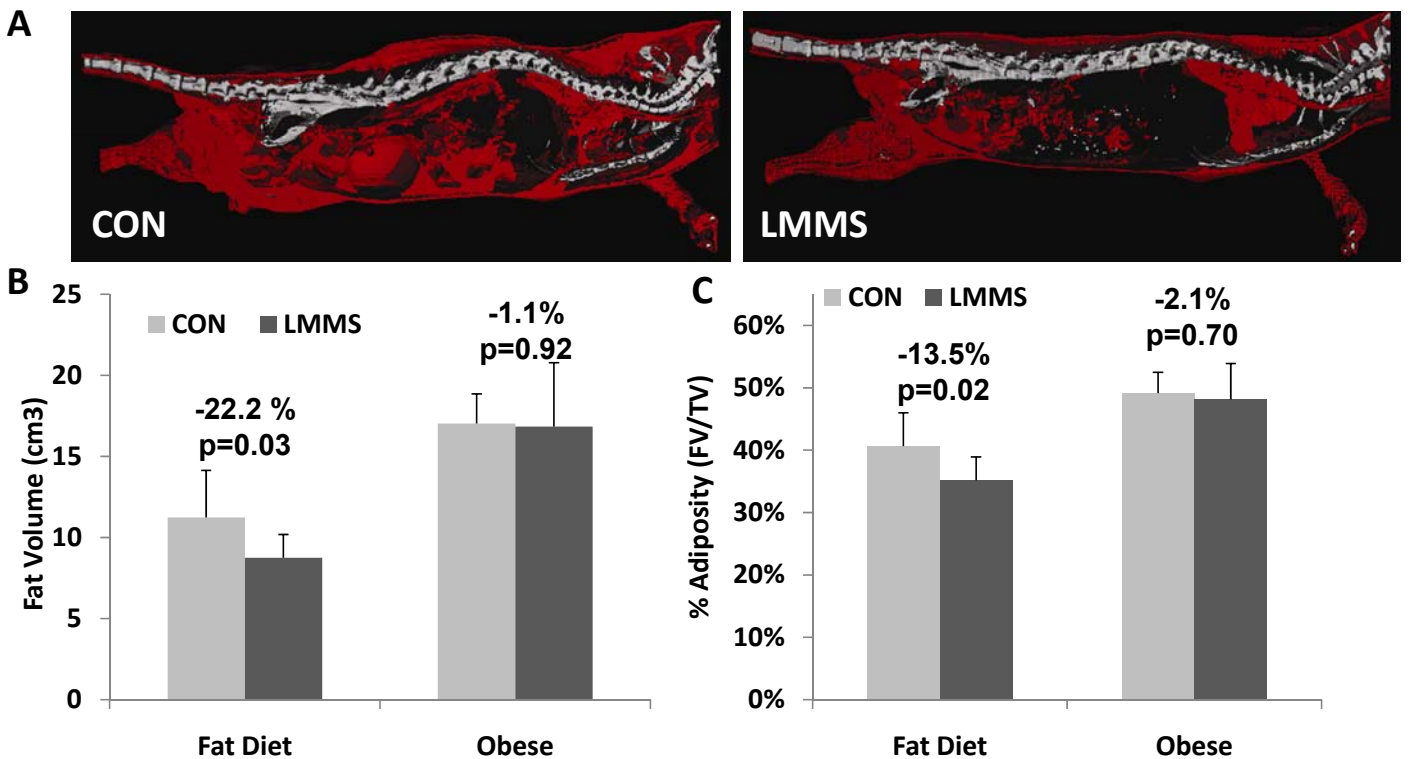
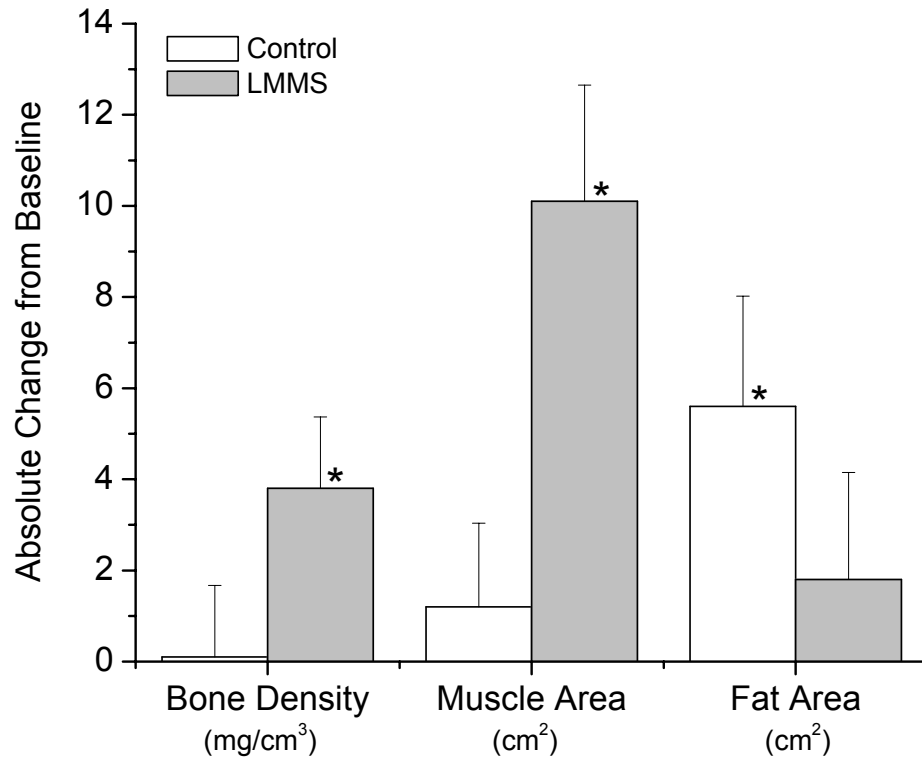


**Figure 7.** As measured by CT scans in the lumbar region of the spine, a group of young osteopenic women subject to LMMS for 12 months (n=24; gray bars  $\pm$  s.e.) increased both trabecular bone density (p=0.03 relative to baseline; mg/cm<sup>3</sup>) and area of paraspinous muscle (p<0.001; cm<sup>2</sup>), changes paralleled by a non-significant increase in visceral fat formation (p=0.22; cm<sup>2</sup>). Conversely, women in the CON group (n=24; white bars  $\pm$  s.e.), while failing to increase either bone density (p=0.93) or muscle area (p=0.52), realized a significant increase in visceral fat formation (p=0.015). \* are significantly different from baseline.



## Reference List

1. Gesta,S., Tseng,Y.H., & Kahn,C.R. Developmental origin of fat: tracking obesity to its source. *Cell* **131**, 242-256 (2007).
2. Ghosh,K. & Ingber,D.E. Micromechanical control of cell and tissue development: Implications for tissue engineering. *Adv. Drug Deliv. Rev.*(2007).
3. Rehfeldt,F., Engler,A.J., Eckhardt,A., Ahmed,F., & Discher,D.E. Cell responses to the mechanochemical microenvironment-Implications for regenerative medicine and drug delivery. *Adv. Drug Deliv. Rev.*(2007).
4. Rosen,E.D. & MacDougald,O.A. Adipocyte differentiation from the inside out. *Nat. Rev. Mol. Cell Biol.* **7**, 885-896 (2006).
5. Song,H.Y., Jeon,E.S., Kim,J.I., Jung,J.S., & Kim,J.H. Oncostatin M promotes osteogenesis and suppresses adipogenic differentiation of human adipose tissue-derived mesenchymal stem cells. *J Cell Biochem.*(2007).
6. De,C.P. *et al.* Rosiglitazone modifies the adipogenic potential of human muscle satellite cells. *Diabetologia* **49**, 1962-1973 (2006).
7. Lazarenko,O.P. *et al.* Rosiglitazone Induces Decreases in Bone Mass and Strength that Are Reminiscent of Aged Bone. *Endocrinology* **148**, 2669-2680 (2007).
8. Crossno,J.T., Jr., Majka,S.M., Grazia,T., Gill,R.G., & Klemm,D.J. Rosiglitazone promotes development of a novel adipocyte population from bone marrow-derived circulating progenitor cells. *J Clin. Invest* **116**, 3220-3228 (2006).
9. Song,G. *et al.* Mechanical stretch promotes proliferation of rat bone marrow mesenchymal stem cells. *Colloids Surf. B Biointerfaces.*(2007).
10. David,V. *et al.* Mechanical loading down-regulates peroxisome proliferator-activated receptor gamma in bone marrow stromal cells and favors osteoblastogenesis at the expense of adipogenesis. *Endocrinology* **148**, 2553-2562 (2007).
11. Dazzi,F. & Horwood,N.J. Potential of mesenchymal stem cell therapy. *Curr. Opin. Oncol.* **19**, 650-655 (2007).
12. Mukherjee,S. *et al.* Pharmacologic targeting of a stem/progenitor population in vivo is associated with enhanced bone regeneration in mice. *J. Clin. Invest* **118**, 491-504 (2008).
13. Rubin,C.T. *et al.* Adipogenesis is inhibited by brief, daily exposure to high-frequency, extremely low-magnitude mechanical signals. *Proc. Natl. Acad. Sci. U. S. A.*(2007).
14. Fritton,J.C., Rubin,C.T., Qin,Y.X., & McLeod,K.J. Whole-body vibration in the skeleton: development of a resonance-based testing device. *Ann. Biomed. Eng* **25**, 831-839 (1997).

15. Rubin,C.T. & Lanyon,L.E. Dynamic strain similarity in vertebrates; an alternative to allometric limb bone scaling. *J. Theor. Biol.* **107**, 321-327 (1984).
16. Gilsbach,R., Kouta,M., Bonisch,H., & Bruss,M. Comparison of in vitro and in vivo reference genes for internal standardization of real-time PCR data. *Biotechniques* **40**, 173-177 (2006).
17. Luu,Y.K. *et al.* Determination of Subcutaneous and Visceral Fat Distribution by In Vivo Micro Computed Tomography. *Medical Engineering and Physics* **under review**, (2008).
18. Lublinsky,S., Luu,Y.K., Rubin,C.T., & Judex,S. An Automated Algorithm to Separate Visceral from Subcutaneous Fat in Micro Computed Tomographies. 2008. Ref Type: Unpublished Work
19. Gilsanz,V. *et al.* Low-level, high-frequency mechanical signals enhance musculoskeletal development of young women with low BMD. *J Bone Miner Res* **21**, 1464-1474 (2006).
20. Robert J.Seely *et al.* Application of the Weisberg t-test for Outliers. Pharmaceutical Technology Europe . 2003. Ref Type: Magazine Article
21. Van,V.P., Falla,N., Snoeck,H., & Mathieu,E. Characterization and purification of osteogenic cells from murine bone marrow by two-color cell sorting using anti-Sca-1 monoclonal antibody and wheat germ agglutinin. *Blood* **84**, 753-763 (1994).
22. Li,X. *et al.* Sclerostin binds to LRP5/6 and antagonizes canonical Wnt signaling. *J. Biol. Chem.* **280**, 19883-19887 (2005).
23. Lin,S., Thomas,T.C., Storlien,L.H., & Huang,X.F. Development of high fat diet-induced obesity and leptin resistance in C57Bl/6J mice. *Int. J. Obes. Relat Metab Disord.* **24**, 639-646 (2000).
24. Gimble,J.M., Zvonic,S., Floyd,Z.E., Kassem,M., & Nuttall,M.E. Playing with bone and fat. *J Cell Biochem.* **98**, 251-266 (2006).
25. Hachisuka,H. *et al.* Flow cytometric discrimination of mesenchymal progenitor cells from bone marrow-adherent cell populations using CD34/44/45(-) and Sca-1(+) markers. *J. Orthop. Sci.* **12**, 161-169 (2007).
26. Haylock,D.N. *et al.* Hemopoietic stem cells with higher hemopoietic potential reside at the bone marrow endosteum. *Stem Cells* **25**, 1062-1069 (2007).
27. Akune,T. *et al.* PPARgamma insufficiency enhances osteogenesis through osteoblast formation from bone marrow progenitors. *J. Clin. Invest* **113**, 846-855 (2004).
28. Takada,I., Suzawa,M., Matsumoto,K., & Kato,S. Suppression of PPAR transactivation switches cell fate of bone marrow stem cells from adipocytes into osteoblasts. *Ann. N. Y. Acad. Sci.* **1116**, 182-195 (2007).

29. Hadjiargyrou, M., Rightmire, E.P., Ando, T., & Lombardo, F.T. The E11 osteoblastic lineage marker is differentially expressed during fracture healing. *Bone* **29**, 149-154 (2001).
30. Sul, H.S., Smas, C., Mei, B., & Zhou, L. Function of pref-1 as an inhibitor of adipocyte differentiation. *Int. J. Obes. Relat Metab Disord.* **24 Suppl 4**, S15-S19 (2000).
31. Gregoire, F.M., Smas, C.M., & Sul, H.S. Understanding adipocyte differentiation. *Physiol Rev.* **78**, 783-809 (1998).
32. Koh, Y.J. *et al.* Bone marrow-derived circulating progenitor cells fail to transdifferentiate into adipocytes in adult adipose tissues in mice. *J. Clin. Invest* **117**, 3684-3695 (2007).
33. Scadden, D.T. The weight of cell identity. *J. Clin. Invest* **117**, 3653-3655 (2007).
34. Weisberg, S.P. *et al.* Obesity is associated with macrophage accumulation in adipose tissue. *J Clin. Invest* **112**, 1796-1808 (2003).
35. Despres, J.P. Cardiovascular disease under the influence of excess visceral fat. *Crit Pathw. Cardiol.* **6**, 51-59 (2007).
36. Haffner, S.M. Abdominal adiposity and cardiometabolic risk: do we have all the answers? *Am. J. Med.* **120**, S10-S16 (2007).
37. Haylock, D.N. & Nilsson, S.K. Osteopontin: a bridge between bone and blood. *Br. J. Haematol.* **134**, 467-474 (2006).
38. Gregoire, F.M. Adipocyte differentiation: from fibroblast to endocrine cell. *Exp. Biol. Med. (Maywood.)* **226**, 997-1002 (2001).
39. Lago, F., Dieguez, C., Gomez-Reino, J., & Gualillo, O. Adipokines as emerging mediators of immune response and inflammation. *Nat. Clin. Pract. Rheumatol.* **3**, 716-724 (2007).
40. Duque, G. Will reducing adipogenesis in bone increase bone mass?: PPARgamma2 as a key target in the treatment of age-related bone loss. *Drug News Perspect.* **16**, 341-346 (2003).
41. Liu, H. *et al.* Augmented Wnt signaling in a mammalian model of accelerated aging. *Science* **317**, 803-806 (2007).
42. Astudillo, P., Rios, S., Pastenes, L., Pino, A.M., & Rodriguez, J.P. Increased adipogenesis of osteoporotic human-mesenchymal stem cells (MSCs) characterizes by impaired leptin action. *J. Cell Biochem.* (2007).
43. Zayzafoon, M., Gathings, W.E., & McDonald, J.M. Modeled microgravity inhibits osteogenic differentiation of human mesenchymal stem cells and increases adipogenesis. *Endocrinology* **145**, 2421-2432 (2004).



44. Basso,N., Bellows,C.G., & Heersche,J.N. Effect of simulated weightlessness on osteoprogenitor cell number and proliferation in young and adult rats. *Bone* **36**, 173-183 (2005).
45. Takada,K. *et al.* Treatment of senile osteoporosis in SAMP6 mice by intra-bone marrow injection of allogeneic bone marrow cells. *Stem Cells* **24**, 399-405 (2006).
46. Conboy,I.M. *et al.* Rejuvenation of aged progenitor cells by exposure to a young systemic environment. *Nature* **433**, 760-764 (2005).
47. Schonfeld-Warden,N. & Warden,C.H. Pediatric obesity. An overview of etiology and treatment. *Pediatr. Clin. North Am.* **44**, 339-361 (1997).
48. Eckel,R.H. & Krauss,R.M. American Heart Association call to action: obesity as a major risk factor for coronary heart disease. AHA Nutrition Committee. *Circulation* **97**, 2099-2100 (1998).